

John M Edwards *
Met Office, U.K.

1. INTRODUCTION

Over the past two decades much effort has been devoted to the retrieval of land surface temperature (LST) from the infra-red channels of various satellite instruments. Most current algorithms are based on the generalized split-window approach (Wan and Dozier 2006), wherein the LST is obtained from a semi-empirical regression using two window channels. A accuracy of 1–2 K is typically estimated for such algorithms (Sun and Pinker 2003, Sun et al. 2006, Inamdar et al. 2008). Retrievals are possible only under clear skies, necessitating the use of a cloud-screening algorithm.

The Spin-Enhanced Visible and Infra-Red Imager (SEVIRI) is mounted on the geostationary satellite Metosat-8, which is positioned just east of the prime meridian. Land surface temperatures are routinely retrieved from SEVIRI for the regions of Europe, northern and southern Africa and South America at a temporal resolution of 15 minutes and a spatial resolution of 3 km at nadir and are available from the Land Surface Satellite Application Facility (<http://landsaf.meteo.pt>). More discussion of the algorithms used for this product is given by Caselles et al. 1997 and Trigo et al. 2009a.

Numerical weather forecasts at the Met Office are made using a single Unified Model (MetUM). This can be run in a global configuration or at higher spatial resolution over smaller domains. A *North Atlantic European* (NAE) version of the model, with a resolution of 12 km is run to produce forecasts on ranges of up to 2 days (in addition to higher resolution configurations covering the United Kingdom itself). Whilst sea-surface temperature and synoptic observations of near-surface air temperatures are used in data assimilation, land surface temperatures are not currently assimilated. LSTs therefore provide an independent source of data for assessing the performance of the model's surface and boundary layer schemes.

*Corresponding author address: John M Edwards, Met Office, FitzRoy Road, Exeter, Devon, EX1 3PB, U.K.; email:john.m.edwards@metoffice.gov.uk

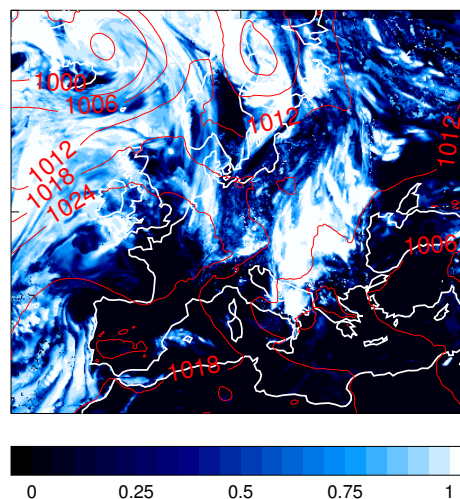


Figure 1: The forecast cloud cover and contours of mean sea-level pressure (hPa) at 12 UTC on the 22nd July 2008.

Since retrievals cannot be performed in the presence of cloud, while the model's LST will be significantly affected by any deficiencies in the forecasting of cloud, initial studies have been directed towards cases where cloud occurred neither in the forecast nor in reality over the length of the forecast. Here comparisons are presented between forecast and retrieved LSTs in conjunction with comparisons between forecast and observed near-surface air temperatures.

2. THE BOUNDARY LAYER AND SURFACE SCHEMES IN THE METUM

The boundary layer scheme in the MetUM is described by Lock (2000) and operates differently in stable and unstable conditions. In unstable conditions, profiles of diffusivities driven from the surface or the tops of boundary layer clouds are imposed: the scheme also includes a representation of non-gradient fluxes. In stable conditions a local mixing scheme is

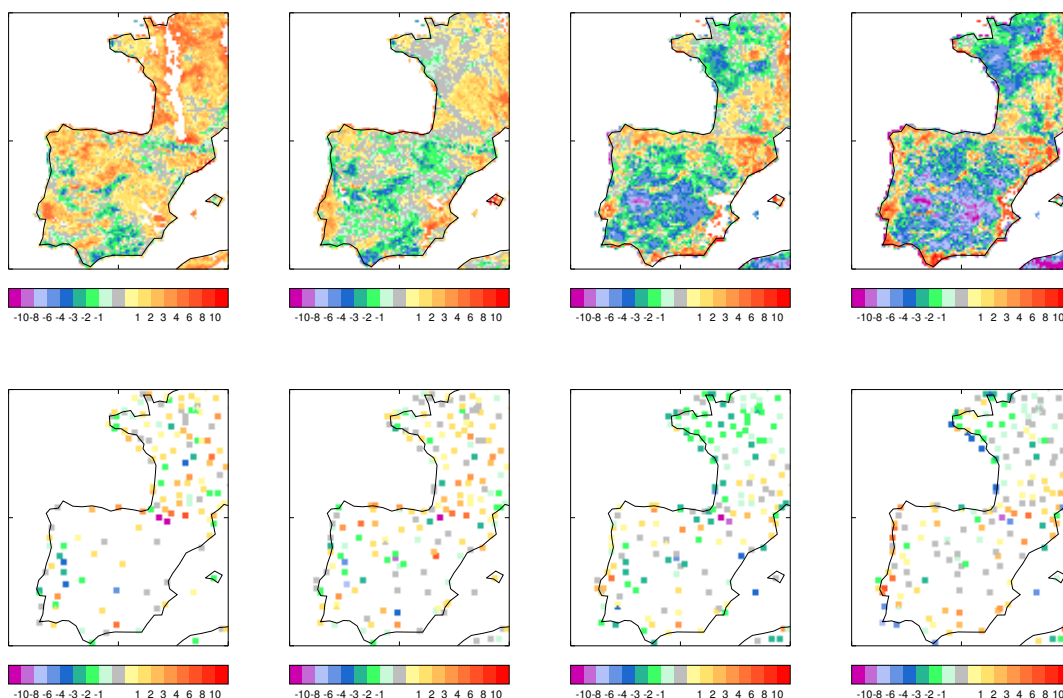


Figure 2: The difference between the forecast and retrieved LSTs and NSTs (K) on the 22nd July 2008. Top row: differences in LST at 00, 06, 09 and 12 UTC. Bottom row: Differences in the NST at 00, 06, 09 and 12 UTC.

used, with the diffusivity depending on the Richardson number. At the time of these studies, the NAE configuration had a resolution of 12 km with 38 vertical levels, 13 of which lay below 3 km, the height up to which the boundary layer scheme is allowed to operate.

The surface scheme is discussed by Essery (2003) and Best (2004) and involves the division of the surface into 9 tiles, based on the occurrence of different types of vegetated or non-vegetated surface. The surface energy budget is calculated separately on each tile, with 4 soil levels, and the exchanges with the atmosphere are calculated using the similarity functions of Beljaars (1991), which are also used to calculate near-surface air temperatures (1.5 m above the surface), since the lowest atmospheric grid-level is 20 m above the surface.

3. CASE 1: 22ND JULY 2008

On this date western Europe lay under an area of high pressure and examination of MODIS imagery revealed an almost total absence of cloud cover over western France and Spain. Figure 1 shows the forecast cloud cover and contours of PMSL at 12 UTC

on this day (12 hours into the forecast), showing that the model also forecast clear skies. The top row of Figure 2 shows the differences between the forecast and retrieved LSTs at 00, 06, 09 and 12 UTC on this day. Retrieved LSTs have been used only where their estimated uncertainty is less than 2 K. Generally, the model shows a small apparent warm bias at 00 UTC (although it should be cautioned that this is close to the allowed uncertainty of the retrievals and that comparison with *in situ* observations (Trigo et al. 2009b) provides some evidence of slight cold biases in the SEVIRI retrievals at night). By 06 UTC, the forecast and the retrievals are in close agreement over western France, but a cold bias begins to develop over Iberia. During the ensuing 6 hours this cold bias intensifies and can amount to as much as 10 K by noon.

The bottom row of the figure shows the differences between the forecast and observed near-surface air temperatures (NSTs) at synoptic observing sites. At 00 UTC, apart from a group of stations in eastern Portugal which exhibit cold biases, the forecast and observed NSTs over Iberia agree rather closely. More significant warm biases are seen over western France, echoing the signal seen in the LSTs. At 06 UTC the

position is largely similar. By 09 UTC there is a broad area of cold NSTs over north-western France, largely in agreement with the signal seen in the LST, but differences over Iberia are less consistent. At 12 UTC the agreement between the model and the observations at most sites is better than 1 K and there is no analogue of the pronounced cold biases seen in the LSTs. Whilst Trigo et al. 2009b suggest that the retrievals may have a warm bias in the daytime, the magnitude of the differences in LST suggests not only that the forecast LST is too cold, but that the magnitude of the difference between the LST and the NST is underestimated in the model.

4. CASE 2: 17TH FEBRUARY 2008

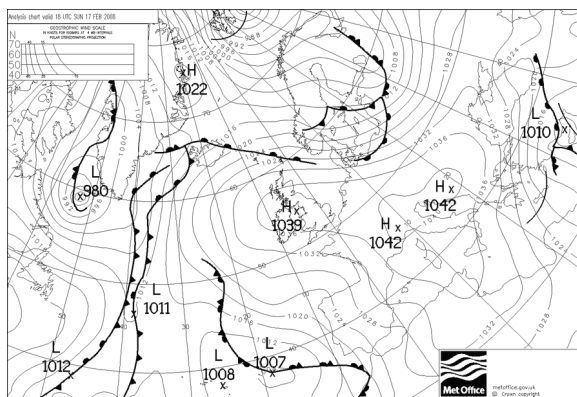


Figure 3: The pressure at mean sea level at 18 UTC on 17th of February 2008.

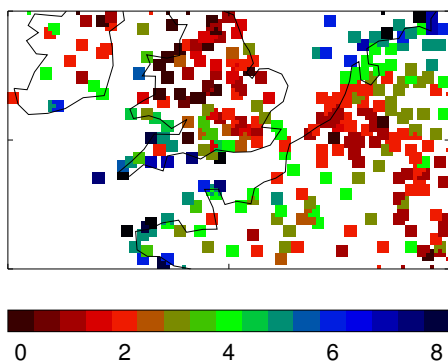


Figure 4: The observed 10-m winds at 16 UTC on the 17th of February 2008.

In winter prolonged periods of extensive clear skies are associated with large anticyclonic pressure systems. In the middle of February 2008 such a system

lay across much of north-western and central Europe. Figure 3 shows the mean sea-level pressure at 18 UTC on the 17th of February. On this day clear skies were forecast and observed over southern England, northern France and the Low Countries and winds were very light (Figure 4). Figure 5 shows differences between the forecast and retrieved LSTs at 12, 16 and 17 UTC, where the forecast LSTs have been taken from the forecast starting from 00 UTC on the 17th of February. At 12 UTC the forecast LSTs are generally colder than the retrievals (though in many places the apparent errors are comparable to the uncertainty of the observations). Through the early afternoon the magnitude of the model's apparent cold bias decreases and by 16 UTC the differences between the forecast and retrieved LSTs seldom exceed 1–2 K in either sense. During following hour the retrieved LSTs in the east of the region shown cool by 4–5 K, while the forecast LST cools more rapidly, giving a substantial cold bias by 17 UTC. The bottom row of the figure shows differences between the forecast NSTs and the synoptic observations at the same times. At 12 UTC (12 hours into the forecast) the forecast air temperatures show mild cold biases, but by 16 UTC, the next hour at which synoptic observations are available, significant cold biases have developed over south-eastern England and the Low Countries. To the east of this region the biases reach 5 K and during the next hour increase to as much as 10 K. Throughout this period the cold bias in the NST is 2–3 K larger than that in the LST. This indicates that in the model the difference between the near-surface air temperature and the skin temperature is underestimated and suggests that in reality the surface may have become decoupled. Similar behaviour was also found on the following day.

5. CONCLUSION

Forecast LSTs have been compared with values retrieved from observations made with the SEVIRI instrument. Two cases from contrasting seasons for which cloud cover did not occur, either in the forecast or in reality have been presented. Often the difference between the forecast and the retrieved LST is close to the estimated uncertainty in the retrieval, but the summer case suggests that the forecast LSTs may have significant cold biases around the middle of the day, whilst in winter the LSTs suggest excessive cooling in the model shortly after the evening transition in very light winds. Looking also at the NSTs suggests that in both these cases the forecast underestimates the magnitude of the difference between

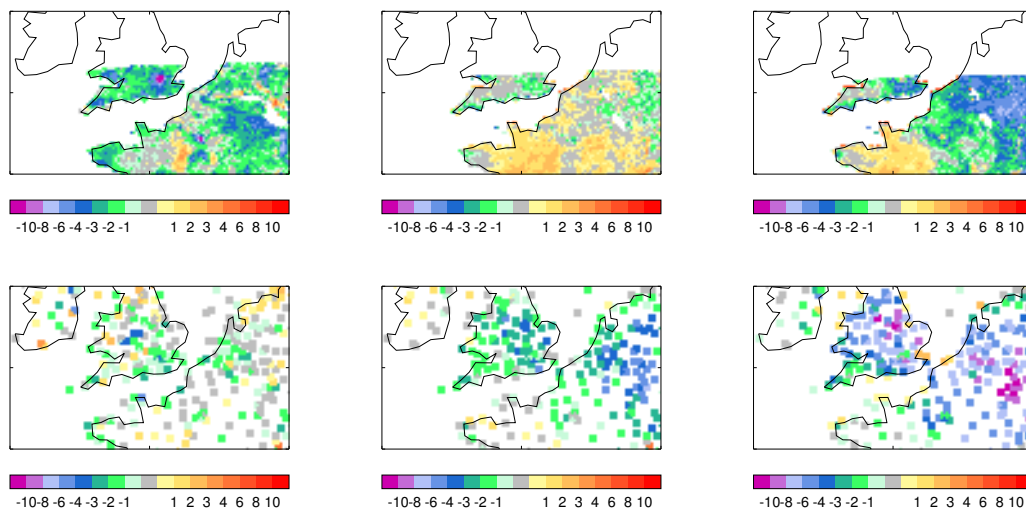


Figure 5: The difference between the forecast and retrieved LSTs and NSTs on the 17th February 2008. Top row: differences in LST at 12, 16 and 17 UTC. Bottom row: Differences in the NST at 12, 16 and 17 UTC.

the NST and the LST.

6. REFERENCES

- Beljaars, A. C. M. and A. A. M. Holtslag, 1991: Flux parametrization over land surfaces for atmospheric models, *J. Appl. Met.*, **30**, pp. 327–341.
- Best, M. J., A. Beljaars, J. Polcher and P. Viterbo, 2004: A proposed structure for coupling tiled surfaces with the planetary boundary layer, *J. Hydrometeorol.*, **5**, pp. 1271–1278.
- Caselles V., E. Valor, C. Coll and E. Rubio, 1997: Thermal band selection for the PRISM instrument 1. Analysis of emissivity-temperature separation algorithms, *J. Geophys. Res.*, bf 102, D10, 11145–11164.
- Essery, R. L. H., M. J. Best, R. A. Betts, P. M. Cox and C. M. Taylor, 2003: Explicit representation of subgrid heterogeneity in a GCM land surface scheme, *J. Hydrometeorol.*, **4**, pp. 530–542.
- Inamdar, A. K., A. French, S. Hook, G. Vaughan and W. Lueckert, 2008: Land surface temperature retrieval at high spatial and temporal resolutions over the southwestern United States, *J. Geophys. Res.*, **113**, D07107, doi:10.1029/2007JD009048.
- Lock, A. P., A. R. Brown, M. R. Bush, G. M. Martin and R. N. B. Smith, 2000: A new boundary layer mixing scheme. Part I: Scheme Description and Single-Column Model Tests, *Mon. Wea. Rev.*, **128**, pp. 3187–3199.
- Sun, D. and R. T. Pinker, 2003: Estimation of land surface temperature from a geostationary operational environmental satellite (GOES-8), *J. Geophys. Res.*, **108(D11)**, pp. 4326, doi:10.1029/2002JD002422.
- Sun, D., R. T. Pinker and M. Kafatos, 2006: Diurnal temperature range over the United States: a satellite view, *Geophys. Res. Lett.*, **33**, pp. L05705, doi:10.1029/2005GL024780.
- Trigo, I., S. Freitas, J. Bioucas-Dias, C. Barroso, I. Monteiro and P. Viterbo, 2009a: Algorithm Theoretical Basis Document for Land Surface Temperature (LST), EUMETSAT LSA SAF, SAF/LAND/IM/ATBD_LST/1.0, pp. 3433–3443.
- Trigo, I. F., I. T. Monteiro, F. Olesen and E. Kabisch, 2009b: An assessment of remotely sensed land surface temperature *J. Geophys. Res.*, bf 113, D17108, doi:10.1029/2008JD010035.
- Wan, Z., J. Dozier, 1996: A generalised split-window algorithm for retrieving land-surface temperature from space, *IEEE Trans. Geosci. Remote Sens.*, vol. **34**, no. 34, pp. 892–905.